Journal of Physics: Conference Series **181** (2009) 012023 doi:10.1088/1742-6596/181/1/012023

Untwisting the Campbell diagrams of weakly anisotropic rotor systems

Oleg N. Kirillov

Dynamics and Vibration Group, Technische Universität Darmstadt, Hochschulstr. 1, D-64289 Darmstadt, Germany

E-mail: kirillov@dyn.tu-darmstadt.de

Abstract. A brake can be modeled as an axi-symmetric rotor perturbed by dissipative, conservative, and non-conservative positional forces originated at the frictional contact with the anisotropic stator. The Campbell diagram of the unperturbed system is a mesh-like structure in the frequency-speed plane with double eigenfrequencies at the nodes. The diagram is convenient for the analysis of the traveling waves in the rotating elastic continuum. Computing sensitivities of the doublets we find that at every particular node the untwisting of the mesh into the branches of complex eigenvalues is generically determined by only four 2x2 sub-blocks of the perturbing matrix. Selection of the unstable modes that cause self-excited vibrations in the subcritical speed range, is governed by the exceptional points at the corners of the singular eigenvalue surface—'double coffee-filter'—which is typical also in the problems of electromagnetic and acoustic wave propagation in non-rotating anisotropic chiral media. As a mechanical example a model of a rotating shaft is studied in detail.

1. Introduction

It is well known that bending waves can propagate in the circumferential direction of an elastic body of revolution rotating about its axis of symmetry [2, 3, 12, 39]. The frequencies of the waves plotted against the rotational speed are referred to as *the Campbell diagram* [4, 39]. Since the spectrum of a perfect rotationally symmetric rotor at standstill has infinitely many double semi-simple eigenvalues—*the doublet modes*—the Campbell diagram contains the eigenvalue branches originated after the splitting of the doublets by the gyroscopic forces [2]. The branches correspond to simple pure imaginary eigenvalues and intersect each other forming a *spectral mesh* [37] in the frequency-speed plane with the double eigenfrequencies at the nodes [23], Fig. 1(a). Dissipative, conservative, and non-conservative perturbations of the axially symmetric rotor, caused by its contact with the anisotropic stator, generically untwist the spectral mesh of pure imaginary eigenvalues of the Campbell diagram into the separate branches of complex eigenvalues in the $(\Omega, \mathrm{Im}\lambda, \mathrm{Re}\lambda)$-space, see Fig. 1(d). Nevertheless, the eigenvalue branches in the perturbed Campbell diagram can both avoid crossings and cross each other, Fig. 1(e). Moreover, the real parts of the perturbed eigenvalues plotted against the rotational speed—*decay rate plots* [39]—can also intersect each other and inflate into "bubbles", Fig. 1(f). This rather complicated behavior is difficult to predict and even to interpret as it was reported in the studies of numerous mechanical systems, see, e.g, [20, 21, 24, 25, 27, 29, 35, 36, 39, 43, 48]. The present work reveals that the untwisting of the Campbell diagrams is determined by a limited number of singular eigenvalue surfaces.

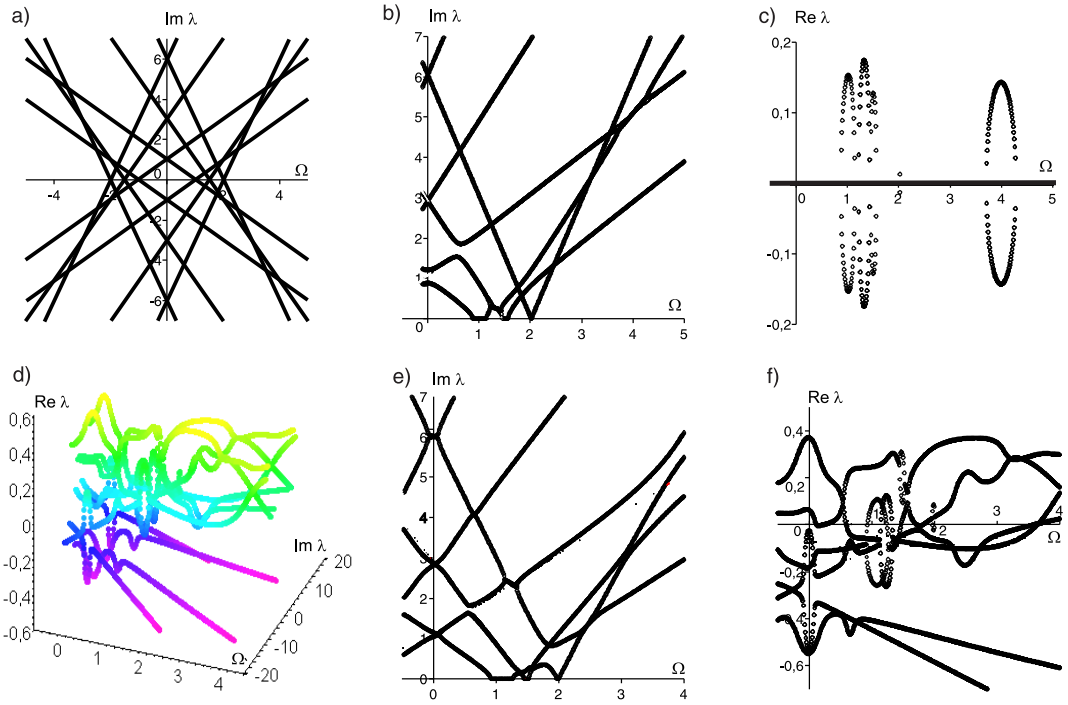

Figure 1. (a) The Campbell diagram of the unperturbed system (2) with 6 d.o.f. in case of $\omega_1 = 1$, $\omega_2 = 3$, and $\omega_3 = 6$; (b) the Campbell diagram and (c) decay rate plots for the stiffness modification $\kappa\mathbf{K}_1$ with $\kappa = 0.2$; (d) untwisting the Campbell diagram in the $(\Omega, \mathrm{Im}\lambda, \mathrm{Re}\lambda)$-space due to perturbation with the matrices $\mathbf{K} = \mathbf{K}_1$, $\mathbf{D} = \mathbf{D}_1$, $\mathbf{N} = \mathbf{N}_1$ and $\kappa = 0.2$, $\delta = 0.1$, and $\nu = 0.2$, (e) the corresponding Campbell diagram and (f) decay rate plots.

2. A model of a weakly anisotropic rotor system

In general, the imperfections in the rotor and stator complicate the linearized equations of motion making them non-self-adjoint with time-dependent coefficients [39]. Nevertheless, an axially symmetric rotor with an anisotropic stator as well as an asymmetric rotor with an isotropic stator are autonomous non-conservative gyroscopic systems [39]. Neglecting the centrifugal stiffness without loss of generality, we consider the finite-dimensional anisotropic rotor system

$$\ddot{\mathbf{x}} + (2\Omega\mathbf{G} + \delta\mathbf{D})\dot{\mathbf{x}} + (\mathbf{P} + \Omega^2\mathbf{G}^2 + \kappa\mathbf{K} + \nu\mathbf{N})\mathbf{x} = 0, \tag{1}$$

which is a perturbation of the isotropic one

$$\ddot{\mathbf{x}} + 2\Omega\mathbf{G}\dot{\mathbf{x}} + (\mathbf{P} + \Omega^2\mathbf{G}^2)\mathbf{x} = 0, \tag{2}$$

where $\mathbf{x} = \mathbb{R}^{2n}$, $\mathbf{P}$=diag$(\omega_1^2, \omega_1^2, \omega_2^2, \omega_2^2, \ldots, \omega_n^2, \omega_n^2)$ is the stiffness matrix, $\mathbf{G} = -\mathbf{G}^T$ is the matrix of gyroscopic forces defined as

$$\mathbf{G} = \mathrm{blockdiag}(\mathbf{J}, 2\mathbf{J}, \ldots, n\mathbf{J}), \quad \mathbf{J} = \begin{pmatrix} 0 & -1 \\ 1 & 0 \end{pmatrix}, \tag{3}$$

and the matrices of damping, $\mathbf{D} = \mathbf{D}^T$, stiffness, $\mathbf{K} = \mathbf{K}^T$, and non-conservative positional forces, $\mathbf{N} = -\mathbf{N}^T$, can depend on the rotational speed Ω. The intensity of the perturbation is controlled by the parameters δ, κ, and ν.

At $\Omega = 0$ the eigenvalues $\pm i\omega_s$, $\omega_s > 0$, of the isotropic rotor (2) are double semi-simple with two linearly independent eigenvectors. The sequence of the frequencies ω_s, where s is an integer

index, is usually different for various bodies of revolution. For example, $\omega_s = s$ corresponds to the natural frequency $f_s = \frac{s}{2\pi r}\sqrt{\frac{P}{\rho}}$ of a circular string of radius r, circumferential tension P, and mass density ρ per unit length [25, 27].

Substituting $\mathbf{x} = \mathbf{u}\exp(\lambda t)$ into (2), we arrive at the eigenvalue problem for the operator $\mathbf{L}_0$

$$\mathbf{L}_0(\Omega)\mathbf{u} := (\mathbf{I}\lambda^2 + 2\Omega\mathbf{G}\lambda + \mathbf{P} + \Omega^2\mathbf{G}^2)\mathbf{u} = 0. \tag{4}$$

The block-diagonal structure of the matrices implies eigenvalues of $\mathbf{L}_0$ in the explicit form

$$\lambda_s^+ = i\omega_s + is\Omega, \quad \overline{\lambda_s^-} = -i\omega_s + is\Omega, \quad \lambda_s^- = i\omega_s - is\Omega, \quad \overline{\lambda_s^+} = -i\omega_s - is\Omega, \tag{5}$$

where bar over a symbol denotes complex conjugate. The eigenvectors of λ_s^+ and $\overline{\lambda_s^-}$ are

$$\mathbf{u}_1^+ = (-i, 1, 0, 0, \ldots, 0, 0)^T, \ \mathbf{u}_2^+ = (0, 0, -i, 1, 0, \ldots, 0)^T, \ \ldots \ \mathbf{u}_n^+ = (0, 0, \ldots, 0, 0, -i, 1)^T, \tag{6}$$

where the imaginary unit holds the $(2s-1)$st position in the vector $\mathbf{u}_s^+$. The eigenvectors, corresponding to the eigenvalues λ_s^- and $\overline{\lambda_s^+}$, are simply $\mathbf{u}_s^- = \overline{\mathbf{u}_s^+}$

For $\Omega > 0$, simple eigenvalues λ_s^+ and λ_s^- correspond to the forward and backward traveling waves, respectively, that propagate in the circumferential direction of the rotor. At the angular velocity $\Omega_s^{cr} = \omega_s/s$ the frequency of the sth backward traveling wave vanishes to zero, so that the wave remains stationary in the non-rotating frame. We assume further in the text that the sequence of the doublets $i\omega_s$ has the property $\omega_{s+1} - \omega_s > \Omega_s^{cr}$, which implies the existence of the minimal *critical* speed $\Omega_{cr} = \Omega_1^{cr} = \omega_1$. When the speed of rotation exceeds the critical speed, some backward waves, corresponding to the eigenvalues $\overline{\lambda_s^-}$, travel slower than the disc rotation speed and appear to be traveling forward (reflected waves).

In Fig. 1(a) the mesh of the eigenvalue branches (5) is shown for the 6 d.o.f.-system (2) with the frequencies $\omega_1 = 1$, $\omega_2 = 3$, and $\omega_3 = 6$ that imitate the distribution of the doublets in the spectrum of a circular ring [35]. To illustrate typical untwisting of the Campbell diagram, we plot in Fig. 1(d)-(f) the eigenvalues of the 6 d.o.f.-system (1) with $\kappa = 0.2$, $\delta = 0.1$, $\nu = 0.2$, $\omega_1 = 1$, $\omega_2 = 3$, and $\omega_3 = 6$ for the perturbing matrix $\mathbf{K} = \mathbf{K}_1$, whose non-zero entries are $k_{11} = 1$, $k_{12} = 2$, $k_{13} = 1$, $k_{14} = 2$, $k_{22} = 1$, $k_{23} = 3$, $k_{24} = 4$, $k_{33} = -3$, $k_{44} = -2.5$, $k_{55} = 4$, $k_{66} = 2$, and for the matrices $\mathbf{D} = \mathbf{D_1}$ and $\mathbf{N} = \mathbf{N_1}$, where

$$\mathbf{D}_1 = \begin{pmatrix} -1 & 2 & 1 & 7 & 2 & -2 \\ 2 & 3 & -2 & -4 & 3 & 1 \\ 1 & -2 & 1 & 8 & 2 & 1 \\ 7 & -4 & 8 & 3 & -2 & 3 \\ 2 & 3 & 2 & -2 & 5 & 5 \\ -2 & 1 & 1 & 3 & 5 & 6 \end{pmatrix}, \quad \mathbf{N}_1 = \begin{pmatrix} 0 & -1 & 1 & -1 & -3 & 8 \\ 1 & 0 & 2 & 3 & 2 & 4 \\ -1 & -2 & 0 & 7 & 1 & 3 \\ 1 & -3 & -7 & 0 & 8 & 2 \\ 3 & -2 & -1 & -8 & 0 & 2 \\ -8 & -4 & -3 & -2 & -2 & 0 \end{pmatrix}. \tag{7}$$

In the following we classify and interpret the typical behavior of the eigenvalues of the weakly anisotropic rotor system (1) with the use of the perturbation formula for the double eigenvalues at the nodes of the spectral mesh (5), which we derive in the next section.

3. Perturbation of the doublets

Introducing the indices $\alpha, \beta, \varepsilon, \sigma = \pm 1$ we find that two branches of the spectral mesh $\lambda_s^\varepsilon = i\alpha\omega_s + i\varepsilon s\Omega$ and $\lambda_t^\sigma = i\beta\omega_t + i\sigma t\Omega$ cross each other at $\Omega = \Omega_0$ with the origination of the double eigenvalue $\lambda_0 = i\omega_0$ with two linearly-independent eigenvectors $\mathbf{u}_s^\varepsilon$ and $\mathbf{u}_t^\sigma$, where

$$\Omega_0 = \frac{\alpha\omega_s - \beta\omega_t}{\sigma t - \varepsilon s}, \quad \omega_0 = \frac{\alpha\sigma\omega_s t - \beta\varepsilon\omega_t s}{\sigma t - \varepsilon s}. \tag{8}$$

Let $\mathbf{M}$ be one of the perturbing matrices $\mathbf{D}$, $\mathbf{K}$, or $\mathbf{N}$. In the following, we use the decomposition of the matrix $\mathbf{M} \in \mathbb{R}^{2n\times 2n}$ into n^2 blocks $\mathbf{M}_{st} \in \mathbb{R}^{2\times 2}$, where $s,t = 1,2,\ldots,n$

$$\mathbf{M} = \begin{pmatrix} * & * & * & * & * \\ * & \mathbf{M}_{ss} & \cdots & \mathbf{M}_{st} & * \\ * & \vdots & \ddots & \vdots & * \\ * & \mathbf{M}_{ts} & \cdots & \mathbf{M}_{tt} & * \\ * & * & * & * & * \end{pmatrix}, \quad \mathbf{M}_{st} = \begin{pmatrix} m_{2s-1,2t-1} & m_{2s-1,2t} \\ m_{2s,2t-1} & m_{2s,2t} \end{pmatrix}. \tag{9}$$

Note that $\mathbf{D}_{st} = \mathbf{D}_{ts}^T$, $\mathbf{K}_{st} = \mathbf{K}_{ts}^T$, and $\mathbf{N}_{st} = -\mathbf{N}_{ts}^T$.

We consider a general perturbation of the matrix operator of the isotropic rotor $\mathbf{L}_0(\Omega) + \Delta\mathbf{L}(\Omega)$. The size of the perturbation $\Delta\mathbf{L}(\Omega) = \delta\lambda\mathbf{D}+\kappa\mathbf{K}+\nu\mathbf{N} \sim \varepsilon$ is small, where $\varepsilon = \|\Delta\mathbf{L}(\Omega_0)\|$ is the Frobenius norm of the perturbation at $\Omega = \Omega_0$. For small $\Delta\Omega = |\Omega - \Omega_0|$ and ε the increment to the doublet $\lambda_0 = i\omega_0$ with the eigenvectors $\mathbf{u}_s^\varepsilon$ and $\mathbf{u}_t^\sigma$, is given by the formula $\det(\mathbf{R} + (\lambda - \lambda_0)\mathbf{Q}) = 0$ [33, 34, 44], where the entries of the 2×2 matrices $\mathbf{Q}$ and $\mathbf{R}$ are

$$\begin{aligned} Q_{st}^{\varepsilon\sigma} &= 2i\omega_0(\bar{\mathbf{u}}_s^\varepsilon)^T\mathbf{u}_t^\sigma + 2\Omega_0(\bar{\mathbf{u}}_s^\varepsilon)^T\mathbf{G}\mathbf{u}_t^\sigma, \\ R_{st}^{\varepsilon\sigma} &= (2i\omega_0(\bar{\mathbf{u}}_s^\varepsilon)^T\mathbf{G}\mathbf{u}_t^\sigma + 2\Omega_0(\bar{\mathbf{u}}_s^\varepsilon)^T\mathbf{G}^2\mathbf{u}_t^\sigma)(\Omega-\Omega_0) + i\omega_0(\bar{\mathbf{u}}_s^\varepsilon)^T\mathbf{D}\mathbf{u}_t^\sigma\delta + (\bar{\mathbf{u}}_s^\varepsilon)^T\mathbf{K}\mathbf{u}_t^\sigma\kappa + (\bar{\mathbf{u}}_s^\varepsilon)^T\mathbf{N}\mathbf{u}_t^\sigma\nu. \end{aligned} \tag{10}$$

Calculating the coefficients (10) with the eigenvectors (6) we find the real and imaginary parts of the sensitivity of the doublet $\lambda_0 = i\omega_0$ at the crossing (8) of the branches λ_s^ε and λ_t^σ

$$\begin{aligned} \mathrm{Re}\lambda &= -\frac{1}{8}\left(\frac{\mathrm{Im}A_1}{\alpha\omega_s} + \frac{\mathrm{Im}B_1}{\beta\omega_t}\right) \pm \sqrt{\frac{|c| - \mathrm{Re}c}{2}}, \\ \mathrm{Im}\lambda &= \omega_0 + \frac{\Delta\Omega}{2}(s\varepsilon + t\sigma) + \frac{\kappa}{8}\left(\frac{\mathrm{tr}\mathbf{K}_{ss}}{\alpha\omega_s} + \frac{\mathrm{tr}\mathbf{K}_{tt}}{\beta\omega_t}\right) \pm \sqrt{\frac{|c| + \mathrm{Re}c}{2}}, \end{aligned} \tag{11}$$

where $c = \mathrm{Re}c + i\mathrm{Im}c$ with

$$\begin{aligned} \mathrm{Im}c &= \frac{\alpha\omega_t\mathrm{Im}A_1 - \beta\omega_s\mathrm{Im}B_1}{8\omega_s\omega_t}(s\varepsilon - t\sigma)\Delta\Omega + \kappa\frac{(\alpha\omega_s\mathrm{tr}\mathbf{K}_{tt} - \beta\omega_t\mathrm{tr}\mathbf{K}_{ss})(\alpha\omega_s\mathrm{Im}B_1 - \beta\omega_t\mathrm{Im}A_1)}{32\omega_s^2\omega_t^2} \\ &- \alpha\beta\kappa\frac{\mathrm{Re}A_2\mathrm{tr}\mathbf{K}_{st}\mathbf{J}_{\varepsilon\sigma} - \mathrm{Re}B_2\mathrm{tr}\mathbf{K}_{st}\mathbf{I}_{\varepsilon\sigma}}{8\omega_s\omega_t}, \\ \mathrm{Re}c &= \left(\frac{t\sigma - s\epsilon}{2}\Delta\Omega + \kappa\frac{\beta\omega_s\mathrm{tr}\mathbf{K}_{tt} - \alpha\omega_t\mathrm{tr}\mathbf{K}_{ss}}{8\omega_s\omega_t}\right)^2 + \alpha\beta\frac{(\mathrm{tr}\mathbf{K}_{st}\mathbf{J}_{\varepsilon\sigma})^2 + (\mathrm{tr}\mathbf{K}_{st}\mathbf{I}_{\varepsilon\sigma})^2}{16\omega_s\omega_t}\kappa^2 \\ &- \frac{(\alpha\omega_s\mathrm{Im}B_1 - \beta\omega_t\mathrm{Im}A_1)^2 + 4\alpha\beta\omega_s\omega_t((\mathrm{Re}A_2)^2 + (\mathrm{Re}B_2)^2)}{64\omega_s^2\omega_t^2}. \end{aligned} \tag{12}$$

The complex coefficients A_1, A_2 and B_1, B_2 depend only on those entries of the matrices $\mathbf{D}$, $\mathbf{K}$, and $\mathbf{N}$ that belong to the four 2×2 blocks (9) with the indices s and t

$$\begin{aligned} A_1 &= \delta\lambda_0\mathrm{tr}\mathbf{D}_{ss} + \kappa\mathrm{tr}\mathbf{K}_{ss} + \varepsilon 2i\nu n_{2s-1,2s}, & A_2 &= \sigma\nu\mathrm{tr}\mathbf{N}_{st}\mathbf{I}_{\varepsilon\sigma} + i(\delta\lambda_0\mathrm{tr}\mathbf{D}_{st}\mathbf{J}_{\varepsilon\sigma} + \kappa\mathrm{tr}\mathbf{K}_{st}\mathbf{J}_{\varepsilon\sigma}), \\ B_1 &= \delta\lambda_0\mathrm{tr}\mathbf{D}_{tt} + \kappa\mathrm{tr}\mathbf{K}_{tt} + \sigma 2i\nu n_{2t-1,2t}, & B_2 &= \sigma\nu\mathrm{tr}\mathbf{N}_{st}\mathbf{J}_{\varepsilon\sigma} - i(\delta\lambda_0\mathrm{tr}\mathbf{D}_{st}\mathbf{I}_{\varepsilon\sigma} + \kappa\mathrm{tr}\mathbf{K}_{st}\mathbf{I}_{\varepsilon\sigma}), \end{aligned} \tag{13}$$

where

$$\mathbf{I}_{\varepsilon\sigma} = \begin{pmatrix} \varepsilon & 0 \\ 0 & \sigma \end{pmatrix}, \quad \mathbf{J}_{\varepsilon\sigma} = \begin{pmatrix} 0 & -\sigma \\ \varepsilon & 0 \end{pmatrix}. \tag{14}$$

Therefore, we have identified the elements of the matrices of the perturbation that control the *eigenvalue assignment* [47] near every particular node (Ω_0, ω_0) of the spectral mesh.

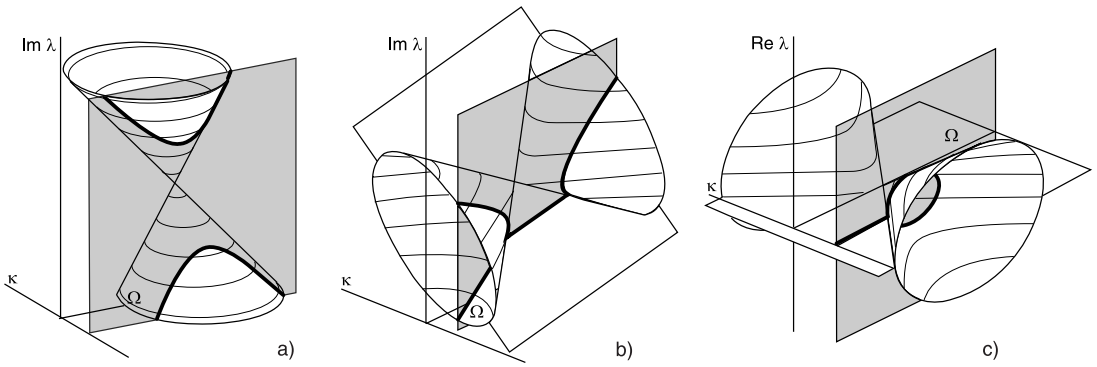

Figure 2. Eigenvalue surfaces (MacKay's cones [15]) and (bold lines) their cross-sections in the plane $\kappa = const$ (grey): (a) a near-vertically oriented cone of imaginary parts in the subcritical range ($\mathrm{Re}\lambda = 0$); (b) imaginary parts forming a near-horizontally oriented cone (15) with the attached membrane (16) and (c) the real parts forming a near-horizontally oriented cone $(\mathrm{Re}\lambda)^2 = -\mathrm{Re}c$ with the attached membrane $\mathrm{Re}\lambda = 0$ in the supercritical speed range.

4. MacKay's eigenvalue cones and instability bubbles due to stiffness modification

Modification of the stiffness matrix induced by the elastic support or by the stationary spring interacting with the rotating continua is typical in the models of rotating shafts [10, 11], computer disc drives [20, 21], circular saws [25, 27, 29], disc brakes [24, 48], and turbine discs [39].

Assuming $\delta = 0$ and $\nu = 0$ in (11) we find that the eigenvalues of the system (5) with the stiffness modification $\kappa\mathbf{K}$ either are pure imaginary ($\mathrm{Re}\lambda = 0$) and form a conical surface in the $(\Omega, \kappa, \mathrm{Im}\lambda)$-space with the apex at the point $(\Omega_0, 0, \omega_0)$, Fig. 2(a),

$$\left(\mathrm{Im}\lambda - \omega_0 - \frac{\kappa}{8}\left(\frac{\mathrm{tr}\mathbf{K}_{ss}}{\alpha\omega_s} + \frac{\mathrm{tr}\mathbf{K}_{tt}}{\beta\omega_t}\right) - \frac{\Omega - \Omega_0}{2}(s\varepsilon + t\sigma)\right)^2 = \mathrm{Re}c \tag{15}$$

or they are complex and in the $(\Omega, \kappa, \mathrm{Re}\lambda)$-space their real parts originate a cone $(\mathrm{Re}\lambda)^2 = -\mathrm{Re}c$ with the apex at the point $(\Omega_0, 0, 0)$, Fig. 2(c). In the $(\Omega, \kappa, \mathrm{Im}\lambda)$-space the corresponding imaginary parts belong to the plane

$$\mathrm{Im}\lambda = \omega_0 + \frac{\kappa}{8}\left(\frac{\mathrm{tr}\mathbf{K}_{ss}}{\alpha\omega_s} + \frac{\mathrm{tr}\mathbf{K}_{tt}}{\beta\omega_t}\right) + \frac{\Omega - \Omega_0}{2}(s\varepsilon + t\sigma), \tag{16}$$

which is attached to the cone (15) as shown in Fig. 2(b).

The existence of eigenvalues with non-zero real part depends on the sign of the product $\alpha\beta$. It is negative only if the crossing in the Campbell diagram is formed by the eigenvalue branch of the reflected wave and by that of either forward- or backward traveling wave. Otherwise, $\alpha\beta > 0$. Due to the property $\omega_{s+1} - \omega_s > \Omega_s^{cr}$ the crossings of the reflected wave with the forward- and backward traveling waves occur only in the *supercritical* speed range $|\Omega| \geq \Omega_{cr}$. The crossings with $\alpha\beta > 0$ are situated in both the super- and *subcritical* ($|\Omega| < \Omega_{cr}$) ranges. Therefore, the eigenvalues with non-zero real part originate only near the supercritical crossings of the eigenvalue branches λ_s^{ε} and λ_t^{σ} with $\alpha\beta < 0$, when the parameters in the (Ω, κ)-plane are in the sector $\mathrm{Re}c < 0$ bounded by the straight lines $\mathrm{Re}c = 0$

$$\kappa = \frac{4(s\varepsilon - t\sigma)(\Omega - \Omega_0)}{\frac{k_{2t-1,2t-1}+k_{2t,2t}}{\beta\omega_t} - \frac{k_{2s-1,2s-1}+k_{2s,2s}}{\alpha\omega_s} \pm 2\sqrt{\frac{(\varepsilon k_{2s-1,2t-1}+\sigma k_{2s,2t})^2+(\varepsilon k_{2s-1,2t}-\sigma k_{2s,2t-1})^2}{-\alpha\beta\omega_s\omega_t}}}. \tag{17}$$

Since for $\alpha\beta < 0$ the cones of the real parts $(\mathrm{Re}\lambda)^2 = -\mathrm{Re}c$ are near-horizontally oriented and extended along the κ-axis in the $(\Omega, \kappa, \mathrm{Re}\lambda)$-space, their cross-sections by the planes $\kappa = const$

are ellipses that are symmetrical with respect to the Ω-axis, as shown in Fig. 1(c) and in Fig. 2(c). Since one-half of the ellipse corresponds to the eigenvalues with positive real parts, it is called the *bubble of instability* [15]. Equation (17) is, therefore, a linear approximation to the boundary of the domain of instability, which is divergence (parametric resonance) for $\Omega_0 = \Omega_s^{cr}$ and flutter (combination resonance) otherwise. The near-horizontal orientation of the corresponding cones of imaginary parts (15) in the $(\Omega, \kappa, \mathrm{Im}\lambda)$-space explains deformation in the presence of the perturbation $\kappa\mathbf{K}$ of the crossings with $\alpha\beta < 0$ into the branches of a hyperbola connected by a straight line in the Campbell diagram, see Fig. 1(b) and Fig. 2(b).

Near the crossings with $\alpha\beta > 0$ the perturbed eigenvalues are pure imaginary (stability). The corresponding cones of imaginary parts (15) are near-vertically oriented in the $(\kappa, \Omega, \mathrm{Im}\lambda)$-space, Fig. 2(a). In the plane $\kappa = const$ this yields the *avoided crossing* [15], which is approximated by a hyperbola shown by the bold lines in Fig. 2(a) (cf. Fig. 1(b)).

The conical singularities of the eigenvalue surfaces in the Hamiltonian systems were known already to Hamilton himself, who predicted the effect of conical refraction of light in birefringent crystals [1, 38]. Later on, the conical singularities of eigenvalue surfaces were found in atomic, nuclear, and molecular physics [6, 7, 22]. Nowadays they bear a name of the Hamilton's *diabolical points* [38]. The existence of the two different orientations of the eigenvalue cones is another fundamental fact of stability theory of Hamiltonian systems established by MacKay in [15] and based on the results of Krein, who introduced the notion of the signature of eigenvalues [14].

To evaluate the Krein signatures, we reduce the system (2) to the form $\dot{\mathbf{y}} = \mathbf{A}\mathbf{y}$, where

$$\mathbf{A} = \begin{pmatrix} -\Omega\mathbf{G} & \mathbf{I}_n \\ -\mathbf{P} & -\Omega\mathbf{G} \end{pmatrix} = \mathbf{J}_{2n}\mathbf{A}^T\mathbf{J}_{2n}, \quad \mathbf{J}_{2n} = \begin{pmatrix} 0 & -\mathbf{I}_n \\ \mathbf{I}_n & 0 \end{pmatrix}, \quad \mathbf{y} = \begin{pmatrix} \mathbf{x} \\ \dot{\mathbf{x}} + \Omega\mathbf{G}\mathbf{x} \end{pmatrix}. \tag{18}$$

The Hamiltonian symmetry of the matrix $\mathbf{A}$ implies its self-adjointness in a Krein space with the indefinite inner product $[\mathbf{a}, \mathbf{b}] = \overline{\mathbf{b}}^T\mathbf{J}_{2n}\mathbf{a}, \quad \mathbf{a}, \mathbf{b} \in \mathbb{C}^{2n}$. The matrix $\mathbf{A}$ has the eigenvalues $\lambda_s^{\pm}$ given by the formulas (5) with the eigenvectors

$$\mathbf{a}_s^{++} = \begin{pmatrix} \mathbf{u}_s^+ \\ \lambda_s^+\mathbf{u}_s^+ + \Omega\mathbf{G}\mathbf{u}_s^+ \end{pmatrix}, \quad \mathbf{a}_s^{+-} = \begin{pmatrix} \mathbf{u}_s^- \\ \lambda_s^-\mathbf{u}_s^- + \Omega\mathbf{G}\mathbf{u}_s^- \end{pmatrix}, \tag{19}$$

where the vectors $\mathbf{u}_s^{\pm}$ are determined by expressions (6). Since $i[\mathbf{a}_s^{++}, \mathbf{a}_s^{++}] = i[\mathbf{a}_s^{+-}, \mathbf{a}_s^{+-}] = 4\omega_s > 0$, the eigenvalues λ_s^+ and λ_s^- of the forward and backward traveling waves acquire *positive Krein signature*. The eigenvalues $\overline{\lambda_s^+}$ and $\overline{\lambda_s^-}$ of the reflected waves with $i[\mathbf{a}_s^{-+}, \mathbf{a}_s^{-+}] = i[\mathbf{a}_s^{--}, \mathbf{a}_s^{--}] = -4\omega_s < 0$, have the opposite, *negative Krein signature* [14, 15, 17, 37]. The signature of an eigenvalue in the Campbell diagram coincides with the sign of the doublet at $\Omega = 0$, from which it is branched, and does not change with the variation of Ω. This implies $\alpha\beta > 0$ and near-vertically oriented cones of imaginary parts (15) at the crossings of eigenvalue branches with the *definite* (positive) Krein signature and $\alpha\beta < 0$ and near-horizontally oriented cones of imaginary parts (15) at the crossings with the *mixed* Krein signature [15].

The Krein signature coincides with the sign of the second derivative of the energy, which is a non-degenerate definite quadratic form on the real invariant space associated to a complex conjugate pair of simple pure imaginary non-zero eigenvalues [15]. Interaction of waves with positive and negative energy is a well known mechanism of instability of the moving fluids and plasmas [15, 18]; in rotor dynamics this yields flutter in the supercritical speed range, which is known as the mass and stiffness instabilities [24, 39].

Therefore, in case when anisotropy of the stator is caused by the stiffness modification only, the untwisting of the Campbell diagram is completely described by the one-parameter slices of the two-parameter MacKay's eigenvalue cones. Since there are only two possible spatial orientations of the cones corresponding to either definite or mixed Krein signatures, all one has to do to predict the untwisting of the Campbell diagram into avoided crossings or into bubbles

of instability is to calculate the signatures of the appropriate eigenvalues of the isotropic rotor. In the following, we develop the MacKay's theory further and show that even in the presence of non-Hamiltonian perturbations, all the observed peculiarities of the Campbell diagrams and decay rate plots are the one-parameter slices of the eigenvalue surfaces near a limited number of other singularities associated with the definite and mixed Krein signature of eigenvalues.

5. Double coffee-filter singularity near the crossings with definite Krein signature

Understanding the general rules of untwisting the Campbell diagrams of weakly anisotropic rotor systems in the presence of dissipative and non-conservative perturbations is important for the linear stability analysis and for the interpretation of the numerical data in both low- and high-speed applications [39]. In the latter *supercritical flutter and divergence* instabilities are easily excited just by the Hamiltonian perturbations like stiffness modification near the crossings with the mixed Krein signature. Among the low-speed applications the untwisting of the Campbell diagram is directly related to the onset of friction-induced oscillations in brakes, clutches, paper calenders, and even in musical instruments like the glass harmonica [9, 44, 45, 46, 47, 48, 51]. In contrast to the supercritical instabilities, the excitation of the *subcritical flutter* near the crossings with the definite Krein signature by the Hamiltonian perturbations only, is impossible. In this case the non-Hamiltonian dissipative and circulatory forces are required for destabilization.

In general, dissipative, $\delta\mathbf{D}$, and non-conservative, $\nu\mathbf{N}$, perturbations unfold the MacKay's eigenvalue cones (15) and $(\mathrm{Re}\lambda)^2 = -\mathrm{Re}c$ into the surfaces $\mathrm{Im}\lambda(\Omega,\kappa)$ and $\mathrm{Re}\lambda(\Omega,\kappa)$, described by the formulas (11). The new eigenvalue surfaces have singularities at the *exceptional points* [30, 31, 32] that correspond to the double eigenvalues with the Jordan chain that born after the splitting of the double semi-simple eigenvalue $i\omega_0$ at $\Omega = \Omega_0$. In some works numerical methods were developed to find the coordinates of these singularities [16]. Perturbation of the Hamilton's diabolical points is another efficient way to locate the exceptional points [33, 34, 37, 44]. Indeed, from the condition $c = 0$ we easily find their approximate locations in the (Ω,κ)-plane

$$\Omega^{\pm}_{EP} = \Omega_0 + \kappa^{\pm}_{EP}\frac{4\omega_s\omega_t U - \beta\omega_s \mathrm{tr}\mathbf{K}_{tt} + \alpha\omega_t \mathrm{tr}\mathbf{K}_{ss}}{4\omega_s\omega_t(t\sigma - s\varepsilon)}, \quad \kappa^{\pm}_{EP} = \pm\sqrt{\frac{X^2 + \alpha\beta(Y^2+Z^2)}{U^2+\alpha\beta(V^2+W^2)}}. \tag{20}$$

The coefficients U, V, W and X, Y, Z in (20) are

$$\begin{aligned} U &= \frac{\mathrm{Re}A_2\mathrm{tr}\mathbf{K}_{st}\mathbf{J}_{\varepsilon\sigma} - \mathrm{Re}B_2\mathrm{tr}\mathbf{K}_{st}\mathbf{I}_{\varepsilon\sigma}}{\alpha\omega_s\mathrm{Im}B_1 - \beta\omega_t\mathrm{Im}A_1}, \quad V = \frac{\mathrm{tr}\mathbf{K}_{st}\mathbf{J}_{\varepsilon\sigma}}{2\sqrt{\omega_s\omega_t}}, \quad W = \frac{\mathrm{tr}\mathbf{K}_{st}\mathbf{I}_{\varepsilon\sigma}}{2\sqrt{\omega_s\omega_t}}, \\ X &= \frac{\alpha\omega_s\mathrm{Im}B_1 - \beta\omega_t\mathrm{Im}A_1}{4\omega_s\omega_t}, \quad Y = \frac{\mathrm{Re}A_2}{2\sqrt{\omega_s\omega_t}}, \quad Z = \frac{\mathrm{Re}B_2}{2\sqrt{\omega_s\omega_t}}. \end{aligned} \tag{21}$$

According to (20), the crossings with the definite Krein signature ($\alpha\beta > 0$) always produce a pair of the exceptional points. For example, for pure non-conservative ($\delta = 0$) and pure dissipative ($\nu = 0$) perturbation of the doublets at $\Omega_0 = 0$, formulas (20) read

$$\Omega^{\pm}_{EP,n} = 0, \quad \kappa^{\pm}_{EP,n} = \pm\frac{2\nu n_{2s-1,2s}}{\rho_1(\mathbf{K}_{ss}) - \rho_2(\mathbf{K}_{ss})}; \quad \Omega^{\pm}_{EP,d} = \pm\delta\frac{\mu_1(\mathbf{D}_{ss}) - \mu_2(\mathbf{D}_{ss})}{4s}, \quad \kappa^{\pm}_{EP,d} = 0, \tag{22}$$

where $\rho_{1,2}(\mathbf{K}_{ss})$ are the eigenvalues of the block $\mathbf{K}_{ss}$ of the matrix $\mathbf{K}$ and $\mu_{1,2}(\mathbf{D}_{ss})$ are the eigenvalues of the block $\mathbf{D}_{ss}$ of the matrix $\mathbf{D}$ [51]. In case of the mixed Krein signature ($\alpha\beta < 0$) the exceptional points exist when the radicand in (20) is positive and does not exist otherwise.

Strong influence of the exceptional points on the stability and their relation to the Ziegler's destabilization paradox due to small damping is well recognized [8, 26, 40, 41, 42, 46]. In

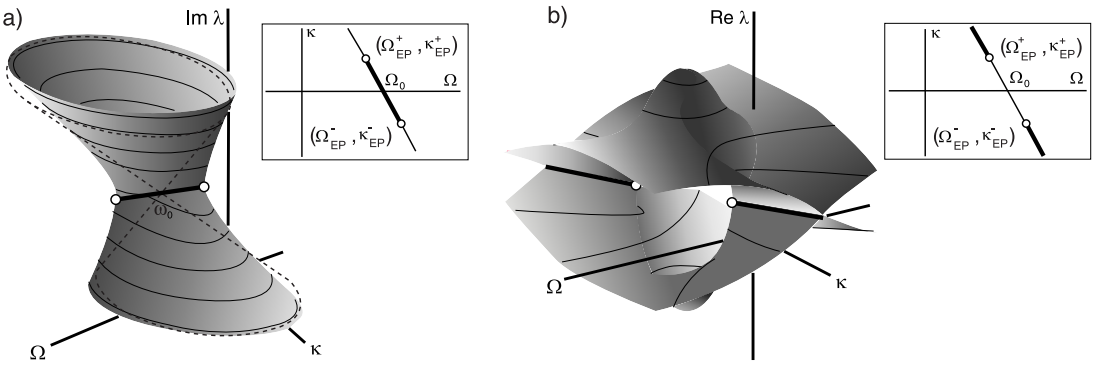

Figure 3. (a) The 'double coffee filter' singular surface $\mathrm{Im}\lambda(\Omega,\kappa)$ with the exceptional points (open circles) and branch cut (bold lines) as a result of the deformation of the MacKay's cone (dashed lines) by the mixed dissipative and circulatory perturbation at any crossing with the definite Krein signature; (b) the corresponding 'viaduct' singular surface $\mathrm{Re}\lambda(\Omega,\kappa)$.

numerous applications in rotor dynamics [20, 21, 24, 25, 27, 29, 39] as well as in hydrodynamics [19], crystal optics [31], acoustics [28], and microwave billiards [30], the generalized crossing scenario in the vicinity of the exceptional points has been observed (visible also in Fig. 1(e,f)) when at the same values of the parameters the imaginary parts of the eigenvalues cross, whereas the real parts don't and vice versa. In our setting, the conditions for coincidence of imaginary parts of the eigenvalues (11) are $\mathrm{Im}c = 0$ and $\mathrm{Re}c \leq 0$ and that for coincidence of the real parts are $\mathrm{Im}c = 0$ and $\mathrm{Re}c \geq 0$. Both real and imaginary parts of the eigenvalues coincide only at the two exceptional points $(\Omega^+_{EP}, \kappa^+_{EP})$ and $(\Omega^-_{EP}, \kappa^-_{EP})$. The segment of the line $\mathrm{Im}c = 0$ connecting the exceptional points is the projection of the branch cut of a singular eigenvalue surface $\mathrm{Im}\lambda(\Omega,\kappa)$. The adjacent parts of the line correspond to the branch cuts of the singular eigenvalue surface $\mathrm{Re}\lambda(\Omega,\kappa)$. Since simultaneous intersection of the different segments of the line $\mathrm{Im}c = 0$ in the (Ω,κ)-plane is not possible one observes the generalized crossing scenario [30, 33, 34] in the planes $(\Omega, \mathrm{Im}\lambda)$ and $(\Omega, \mathrm{Re}\lambda)$ or $(\kappa, \mathrm{Im}\lambda)$ and $(\kappa, \mathrm{Re}\lambda)$.

For example, in case of pure non-conservative perturbation the real parts of the eigenvalues developing near the doublets with the definite Krein signature at $\Omega_0 = 0$ cross each other in the $(\Omega, \mathrm{Re}\lambda)$-plane at the points of the branch cuts $\kappa^2 > (\kappa^{\pm}_{EP,n})^2$

$$\mathrm{Re}\lambda = \pm \frac{2\nu s n_{2s-1,2s}}{(\rho_1(\mathbf{K}_{ss}) - \rho_2(\mathbf{K}_{ss}))\sqrt{\kappa^2 - (\kappa^{\pm}_{EP,n})^2}}\Omega + O(\Omega^3), \tag{23}$$

whereas for $\kappa^2 < (\kappa^{\pm}_{EP,n})^2$ they avoid crossing

$$\mathrm{Re}\lambda = \pm \frac{\rho_1(\mathbf{K}_{ss}) - \rho_2(\mathbf{K}_{ss})}{4\omega_s}\sqrt{(\kappa^{\pm}_{EP,n})^2 - \kappa^2} + O(\Omega^2). \tag{24}$$

At the exceptional points $\kappa = \kappa^{\pm}_{EP,n}$ the eigenvalue branches touch each other at the origin

$$\mathrm{Re}\lambda = \pm \frac{1}{2}\sqrt{\frac{2\nu s n_{2s-1,2s}}{\omega_s}\Omega} + O(\Omega^{3/2}). \tag{25}$$

The degenerate crossing (25) of the real parts has been observed in the model of a rotating circular string passing through the eyelet with friction [25, 44].

Similarly, pure dissipative perturbation of the doublets at $\Omega_0 = 0$ yields crossings of the real parts at the branch cut $\Omega^2 > (\Omega^{\pm}_{EP,d})^2$ in the $(\mathrm{Re}\lambda, \kappa)$-plane and veering of the imaginary parts

$$\mathrm{Im}\lambda = \omega_s \pm s\sqrt{\Omega^2 - (\Omega^{\pm}_{EP,d})^2} + O(\kappa), \;\; \mathrm{Re}\lambda = -\frac{\delta \mathrm{tr}\mathbf{D}_{ss}}{4} \pm \frac{\gamma}{16 s\omega_s \sqrt{\Omega^2 - (\Omega^{\pm}_{EP,d})^2}}\delta\kappa + O(\kappa^3), \quad (26)$$

where $\gamma = 2\mathrm{tr}\mathbf{K}_{ss}\mathbf{D}_{ss} - \mathrm{tr}\mathbf{K}_{ss}\mathrm{tr}\mathbf{D}_{ss}$. At the branch cut $\Omega^2 < (\Omega^{\pm}_{EP,d})^2$ the imaginary parts cross and the real parts avoid crossing

$$\mathrm{Im}\lambda = \omega_s + \frac{\mathrm{tr}\mathbf{K}_{ss}}{4\omega_s}\kappa \pm \frac{\gamma}{16 s\omega_s \sqrt{(\Omega^{\pm}_{EP,d})^2 - \Omega^2}}\delta\kappa + O(\kappa^2), \;\; \mathrm{Re}\lambda = -\frac{\delta \mathrm{tr}\mathbf{D}_{ss}}{4} \pm s\sqrt{(\Omega^{\pm}_{EP,d})^2 - \Omega^2} + O(\kappa^2). \quad (27)$$

At $\Omega = \Omega^{\pm}_{EP,d}$ the crossings of both the real and imaginary parts are degenerate

$$\mathrm{Re}\lambda = -\frac{\delta \mathrm{tr}\mathbf{D}_{ss}}{4} \pm \frac{1}{4}\sqrt{-\delta\kappa\frac{\gamma}{\omega_s}} + O(\kappa^{3/2}), \quad \mathrm{Im}\lambda = \omega_s \pm \frac{1}{4}\sqrt{-\delta\kappa\frac{\gamma}{\omega_s}} + \frac{\mathrm{tr}\mathbf{K}_{ss}}{4\omega_s}\kappa + O(\kappa^{3/2}). \quad (28)$$

The evolving eigenvalue branches reconstruct the eigenvalue surfaces shown in Fig. 3. The qualitative changes of the eigenvalue branches in the one-parameter slices of the surfaces from the crossing to the avoided crossing due to variation of the parameters Ω and κ are caused by the passage through the exceptional points, where the branches touch each other and the eigenvalue surfaces have Whitney's umbrella singularities. The surface of the imaginary parts shown in Fig. 3(a) is formed by the two Whitney's umbrellas with the handles (branch cuts) glued when they are oriented toward each other. This singular surface is known in the physical literature on wave propagation in anisotropic media as the *double coffee filter* [30, 31]. The *viaduct* singular surface of the real parts results from the gluing of the roofs of two Whitney's umbrellas when their handles are oriented outwards, Fig. 3(b). The double coffee filter singularity is a result of the deformation of the MacKay's eigenvalue cone (shown by the dashed lines in Fig. 3(a)) by the dissipative and non-conservative perturbations. These perturbations foliate the plane $\mathrm{Re}\lambda = 0$ into the viaduct singular surface which has self-intersections along the two branch cuts and an ellipse-shaped arch between the two exceptional points, Fig. 3(b). Both types of singular surfaces appear when non-Hermitian perturbation of Hermitian matrices is considered [13, 33, 34].

Therefore, in a weakly non-Hamiltonian system (1) the fundamental qualitative effect of the splitting of the doublets with the definite Krein signature is the origination of the double coffee filter singular surface of the imaginary parts and the viaduct singular surface of the real parts. Structural modification of the matrices of dissipative and non-conservative forces generically does not change the type of the surfaces, preserving the exceptional points and the branch cuts.

6. Example. Rotating shaft

Simplest mechanical examples described by equations (1) and (2) are some two-degrees-of-freedom models of rotating shafts [5, 10, 11, 39]. In [10] the shaft is modeled as the mass m which is attached by two springs with the stiffness coefficients k_1 and $k_2 = k_1 + \kappa$ and two dampers with the coefficients μ_1 and μ_2 to a coordinate system rotating at constant angular velocity Ω, Fig. 4(a). A non-conservative positional force βr acts on the mass. With u and v representing the displacements in the direction of the two rotating coordinate axes, respectively, the system is governed by the equations [10]

$$\begin{aligned} m\ddot{u} + \mu_1\dot{u} - 2m\Omega\dot{v} + (k_1 - m\Omega^2)u + \beta v &= 0, \\ m\ddot{v} + \mu_2\dot{v} + 2m\Omega\dot{u} + (k_2 - m\Omega^2)v - \beta u &= 0. \end{aligned} \quad (29)$$

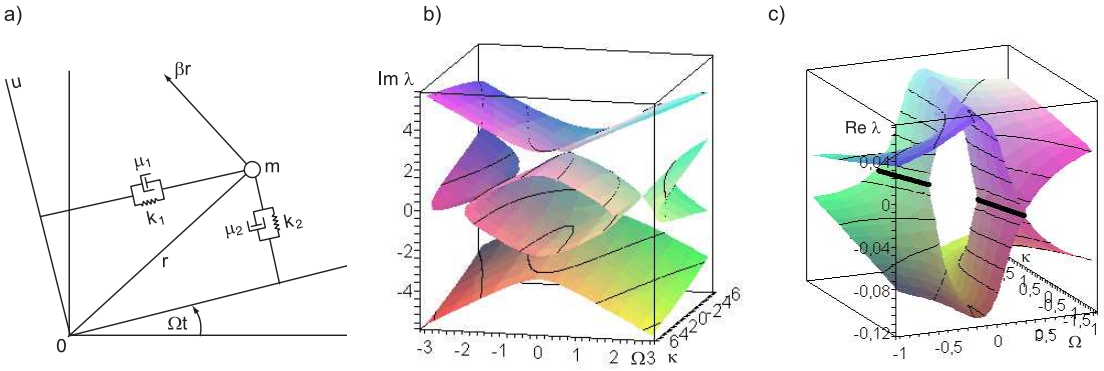

Figure 4. (a) A model of the rotating shaft; (b) four MacKay's cones due to stiffness modification ($\mu_1 = 0$, $\mu_2 = 0$, $\beta = 0$); (c) the viaduct singular surface created by the indefinite damping ($\mu_1 = -0.1$, $\mu_2 = 0.2$) and circulatory force ($\beta = 0.2$).

In Fig. 4(b) we show the numerically found surface of frequencies for the shaft with $m = 1$ and $k_1 = 4$ in the absence of damping and non-conservative forces. The surface has four conical singularities corresponding to the double eigenvalues $\pm 2i$ at $\Omega = 0$ and to the double zero eigenvalues at the critical speeds $\Omega = \pm 2$. The cones in the subcritical speed range are near-vertically oriented while those at the critical speeds are near-horizontal [15]. Consequently, for small stiffness detuning κ the system is stable in the subcritical speed range and unstable by divergence in the vicinity of the critical speeds, where the bubbles of instability in the decay rate plots originate. Addition of the non-conservative forces with $\beta = 0.2$ and indefinite damping with $\mu_1 = -0.1$ and $\mu_2 = 0.2$ yields deformation of the conical surfaces with the apexes at $\Omega = 0$ into the double coffee-filters. The real parts form the viaduct singular surface shown in Fig. 4(c).

7. Conclusion

In the article we aimed at the finding of fundamental properties of a class of non-conservative rotor systems that would unify different linearised models of rotating elastic continua in frictional contact. We have found two types of singular eigenvalue surfaces that exist unavoidably in such models and cannot be destroyed or qualitatively modified by generic changes in the matrices of the system. The double coffee filter and the viaduct singular surface are the imaginary and the real part of the unfolding of any double pure imaginary semi-simple eigenvalue at the crossing of the Campbell diagram with the definite Krein signature. The structure of the perturbing matrices determines only the details of the geometry of the surfaces, such as the coordinates of the exceptional points and the spacial orientation of the branch cuts. It does not yield the qualitative changes irrespective of whether the dissipative and circulatory perturbations are applied separately or in a mixture. For practical applications this means that the behaviour of eigenvalues is described in the same manner for different models of rotor-stator interaction. This will help practitioners and engineers in the development of better models, in their comparison, and in the interpretation of the data both from the numerical and physical experiments. On the other hand, our qualitative results connect the problems of wave propagation in rotating continua with that of electromagnetic and acoustic wave propagation in stationary anisotropic and chiral media [32]. Therefore, the ideas and methods of the latter discipline can be used for more refined investigation of the rotating elastic continua. The qualitative results, the perturbation methodology and the revealed connection to the other physical disciplines can be employed for

the improvement of the existing FEM codes aimed at the modeling and optimization of the elements of rotating machinery.

Acknowledgments
The work has been supported by the research grant DFG HA 1060/43-1.

References

[1] Hamilton W.R. 1833 *Dublin Univ. Rev. Q. Mag.* **1** 795.
[2] Bryan G. 1890 *Proc. Cam. Philos. Soc.* **7** 101.
[3] Lamb H., Southwell R.V. 1921 *Proc. R. Soc. London* A **99** 272.
[4] Campbell W. 1924 *Trans. A.S.M.E.* **46** 31.
[5] Kimball A.L. 1924 *Gen. Elec. Rev.* **27** 244.
[6] Von Neumann J., Wigner E.P. 1929 *Z. Phys.* **30** 467.
[7] Teller E. 1937 *J. Phys. Chem.* **41** 109.
[8] Bottema O. 1956 *Indag. Math.* **18** 403.
[9] Spurr R.T. 1961 *Wear* **4** 150.
[10] Shieh R.C., Masur E.F. 1968 *Z. angew. Math. Phys.* **19** 927.
[11] Crandall S.H. 1970 *J. Sound. Vibr.* **11**(1) 3.
[12] Srinivasan A.V., Lauterbach G.F. 1971 *Trans. ASME. Journal of Engineering for Industry* **93** 1229.
[13] Kahan W. 1975 *Proc. Amer. Math. Soc.* **48** 11.
[14] Krein, M.G. 1983 *Topics in Differential and Integral Equations and Operator Theory* (Birkhäuser, Basel).
[15] MacKay, R.S. 1986 *In: Nonlinear phenomena and chaos, ed. S. Sarkar* (Bristol, Adam Hilger).
[16] Jones C.A. 1988 *Quart. J. Mech. Appl. Math.* **41**(3) 363.
[17] Arnold V.I., Avez A. 1989 *Ergodic Problems of Classical Mechanics* (Addison-Wesley)
[18] Stepanyants Yu.A., Fabrikant A.L. 1989 *Sov. Phys. Uspekhi* **32**(9), 783.
[19] Or A.C. 1991 *Quart. J. Mech. Appl. Math.* **44**(4) 559.
[20] Ono K., Chen J.-S., Bogy D.B. 1991 *Trans. ASME, J. Appl. Mech.* **58** 1005.
[21] Chen J.-S., Bogy D.B. 1992 *Trans. ASME, J. Appl. Mech.* **59** 390.
[22] Mondragon A., Hernandez E. 1993 *J. Phys. A: Math. Gen.* **26** 5595.
[23] Dellnitz M., Melbourne I. 1994 *J. of Comput. and Appl. Math.* **55** 249.
[24] Mottershead J.E., Chan S.N. 1995 *Trans. ASME, J. Vibr. Acoust.* **177** 161.
[25] Yang L., Hutton S.G. 1995 *J. Sound Vibr.* **185** 139.
[26] Hoveijn I., Ruijgrok M. 1995 *Z. angew. Math. Phys.* **46** 384.
[27] Tian J., Hutton S.G. 1999 *Trans. ASME. J. Appl. Mech.* **66** 800.
[28] Shuvalov A.L., Scott N.H. 2000 *Acta Mech.* **140** 1.
[29] Xiong L.G., Chen H., Yi J.M. 2002 *J. Mater. Proc. Techn.* **129** 534.
[30] Keck F., Korsch H.J., Mossmann S. 2003 *J. Phys. A: Math. Gen.* **36** 2125.
[31] Berry M.V., Dennis M.R. 2003 *Proc. R. Soc. Lond.* A **459** 1261.
[32] Berry M.V. 2004 *Czech. J. Phys.* **54** 1039.
[33] Kirillov O.N., Mailybaev A.A., Seyranian A.P. 2005 *J. Phys. A: Math. Gen.* **38** 5531.
[34] Kirillov O.N., Mailybaev A.A., Seyranian A.P. 2005 *Dokl. Phys.* **50** 577.
[35] Canchi S.V., Parker R.G. 2006 *J. Sound. Vibr.* **293** 360.
[36] Young T.H., Lin C.Y. 2006 *J. Sound. Vibr.* **298** 307.
[37] Günther U., Kirillov O.N. 2006 *J. Phys. A: Math. Gen.* **39** 10057.
[38] Berry M.V., Jeffrey M.R. 2007 *In: Progress in Optics, 50, E. Wolf, ed.* (Elsevier).
[39] Genta G. 2007 *Dynamics of rotating systems* (Springer)
[40] Kirillov O.N. 2007 *Intern. J. of Non-Lin. Mech.* **42** 71.
[41] Krechetnikov R., Marsden J.E. 2007 *Rev. Mod. Phys.* **79** 519.
[42] Kirillov O.N. 2007 Dokl. Math. **76**(2) 780.
[43] Lesaffre N., Sinou J.-J., Thouverez F. 2007 *Eur. J. Mech. - A/Sol.* **26**(3), 541.
[44] Kirillov O.N. 2008 *Proc. R. Soc.* A **464** 2321.
[45] Kang J., Krousgrill C.M., Sadeghi F. 2008 *J. Sound Vibr.* **316** 164.
[46] Chevillot F., Sinou J.-J., Mazet G.-B., Hardouin N. and Jézéquel L. 2008 *Arch. Appl. Mech.* **78**, 949.
[47] Ouyang H. 2008 *Mechanical Systems and Signal Processing*, doi: 10.1016/j.ymssp.2008.08.001
[48] Spelsberg-Korspeter G., Hochlenert D., Kirillov O.N., Hagedorn P. 2009 *Trans. ASME, J. Appl. Mech.* **76**.
[49] Kirillov O.N. 2009 *Physics Letters A* **373**(10), 940.
[50] Kirillov O.N., Günther U., Stefani F. 2009 *Phys. Rev. E.* **79**(1) 016205.
[51] Kirillov O.N. 2009 *Int. J. of Vehicle Design* **49**(1)